JOURNAL OF APPLIED ELECTROCHEMISTRY 23 (1993) 693–706

Role of dissolution of Mn(III) species in discharge and recharge of chemically-modified MnO_2 battery cathode materials

D. Y. QU, B. E. CONWAY, L. BAI

Chemistry Department, University of Ottawa, Ottawa, Canada, K1N 6N5

Y. H. ZHOU*, W. A. ADAMS

Electrochemical Science and Technology Centre, University of Ottawa, Ottawa, Canada, K1N 6N5

Received 7 July 1992; revised 9 September 1992

Various experimental techniques, including cyclic-voltammetry, constant current discharge and recharge, with a detecting electrode for determination of soluble Mn(III) intermediate species, were used to study the reaction mechanism involved in the reduction of a chemical modified form of MnO_2 that is multiply rechargeable. The results show how dissolution of Mn(III) species plays an important role in the overall path of the reduction reaction and also in the rechargeability of the material. Mainly an heterogeneous reduction mechanism is involved; substantial loss of capacity can arise if diffusion of the soluble Mn(III) species into the bulk electrolyte solution is allowed to take place. In practical cells, this effect must be minimized using cells with 'starved electrolyte', i.e. with only a small free volume-fraction of KOH electrolyte in the MnO_2-carbon electrode structure. Soluble Mn(III) species were detected in *in situ* experiments by means of (a) a spectro-electrochemical procedure, (b) a 'collector' electrode system at which dissolved Mn(III) was reoxidized to MnO_2, and (c) a rotating ring-disc electrode.

1. Introduction and review

The unique performance characteristics and favourable cost makes the alkaline MnO_2 battery widely applicable and the incentive for converting it into a rechargeable system, extremely appealing. The incentives are connected not only with energetics, material savings and environmental reasons but also with the possibility of entering the vast market of small rechargeable power sources for emergency power, telephone remote communication, photographic equipment and other portable appliances; these applications are dominated now by the more expensive and more toxic lead-acid and nickel/cadmium batteries. Successful development of rechargeable MnO_2-based batteries, including the Zn/MnO_2 system in aqueous solution and Li/MnO_2 in non-aqueous solutions, is of interest for almost all of the present applications of both primary and secondary batteries, while aqueous embodiments, suitable for electric vehicle applications, can be expected in the foreseeable future when/if appropriate energy and power densities are realized.

Manganese dioxides are used extensively as active cathode materials in Léclanche or alkaline Zn/MnO_2 cells. The cathodic and anodic mechanisms of operation of several kinds of MnO_2 have been widely studied by various methods and techniques, as well as the rechargeability of manganese dioxides, especially in alkaline electrolyte, e.g. as in previous works [1, 2].

For the discharge of MnO_2 in alkaline electrolytes, the mechanism proposed by Kozawa, Yeager and Powers [3–9] is now widely adopted. They postulated a two-step mechanism for the reduction of γ-MnO_2 in alkaline solution. The first step is reduction from MnO_2 to $MnO_{1.5}$ (MnOOH) and the second step from $MnO_{1.5}$ to $MnO_{1.0}$ [$Mn(OH)_2$]. In the first step, which was called the 'electron-proton mechanism', the potential kept decreasing. According to Vetter's thermodynamic treatment [10], a potential varying with composition indicates homogeneous phase reduction, as with Li^+ ion intercalation, while when the potential remains constant over a given range of composition, an heterogeneous, two-phase system at equilibrium is indicated. Hence, in the Vetter-type mechanisms the solid phase must be homogeneous and Mn(IV) and Mn(III) states are co-existent, as in an homogeneous redox reaction. The process can be formulated as

$$MnO_2 + H_2O + e^- \longrightarrow MnOOH + OH^-$$

in which electrons and protons are transferred into the lattice of MnO_2.

* Present address: Chemistry Department, Wuhan University, Wuhan 430072, People's Republic of China.

0021-891X

The present and other work [11] reveals the involvement of Mn^{3+} ions or Mn(III) complexes as intermediates which are soluble and are introduced into the electrolyte solution phase upon discharge or recharge.

Because of the introduction of the proton and addition of the first electron, the original MnO_2 lattice expands. At this point, the product, α-MnOOH (recently, δ-MnOOH was suggested according to an X-ray diffraction study [38]) can be recharged back to γ-MnO_2. The second step, which is to be regarded as an heterogeneous phase reduction, is believed to be a 'dissolution-precipitation' type of mechanism involving an Mn(III) complex ion in solution; the reaction mechanism of this second step involves the following stages [4]: (i) dissolution of a complex Mn(III) ion from MnOOH, originating by reduction of the MnO_2; (ii) diffusion of Mn(III) ion species onto the graphite surface; (iii) charge transfer between the electrode and the Mn species; and (iv) precipitation of $Mn(OH)_2$ on or in the porous graphite structure.

The solubility of Mn(III) and Mn(II) species was studied directly by Kozawa, Kalnoki-Kis and Yeager [11] by the polarographic method in various concentrations of KOH; in 9 M KOH, the solubilities of these species are 4.4×10^{-3} M and 4.0×10^{-4} M, respectively, i.e. the solubility of Mn(III) is ten times higher than that of Mn(II). (In this strong KOH the Mn(III) is in the form of $[Mn(OH)_6]^{3-}$ [12]).

Supporting Kozawa's mechanism, using an ultrathin electrolytic cell, a microscope for direct observation and an extraordinarily low-speed cyclic voltammetry (CV) ($180\,mV\,h^{-1}$) technique, Ruetschi [13] observed morphological changes of γ-MnO_2 particles during discharge in various electrolytes and several reduction peaks in the CV. Associated with the first peak, a change in the shape of the original MnO_2 particles was observed. However, sudden dissolution of the grains started during the descending branch of the peak; finally, only the bare substrate remained.

Associated with the second peak, small hexagonal platelets of $Mn(OH)_2$ crystallized out from solution onto the substrate. It is this kind of recrystallized $Mn(OH)_2$ that cannot be reoxidized to the original form of γ-MnO_2.

McBreen [14] proposed a more detailed reaction pathway for the cathodic reduction of γ-MnO_2 and the anodic reoxidation processes, based on data obtained in low sweep-rate cyclic voltammetry ($25\,\mu V\,s^{-1}$) studied in conjunction with X-ray diffraction examination of the structures of the reaction products at various potentials; his results can be summarized in terms of the following steps:

(i) Protons are incorporated into γ-MnO_2 lattice causing lattice dilation and the formation of an amorphous phase (α-MnOOH);

(ii) Further reduction, resulting in conversion of the amorphous phase to $Mn(OH)_2$;

(iii) Oxidation of $Mn(OH)_2$, resulting in the formation of a mixture of γ-Mn_2O_3, γ-MnOOH and β-MnOOH, on recharge,

(iv) Further oxidation yielding δ-MnO_2 with reduction of δ-MnO_2 yielding Mn_3O_4; this Mn_3O_4 cannot be electrochemically oxidized but is reducible to $Mn(OH)_2$ which is then reoxidizable to δ-MnO_2.

Many other studies have also been reported on the mechanisms of MnO_2 reduction [15–21] and the reoxidation processes [22, 23] involving reduced MnO_2.

Various attempts have been made to make the alkaline manganese dioxide cell rechargeable. Significant progress has been made by Kordesh and coworkers [24–26]. According to the proposed mechanism, only α-MnOOH, which is the product of the homogeneous process of γ-MnO_2 reduction, can be reoxidized back to its original form, γ-MnO_2. Hence, Kordesch's method of making the MnO_2 battery system 'rechargeable' is to limit the depth of discharge to less than $MnO_{1.5}$ simply by means of restricting the anode capacity, i.e. the cell is 'anode limited'. In order to minimize dilation of the lattice in the process of introduction of the proton, pressure was used to restrict the expansion of the manganese dioxide electrode during discharge. Because, in the Kordesch type of battery, only one third or less of one electron per Mn atom is practically available to be used, the energy density is relatively low and limitation of the depth of discharge is inconvenient to users.

In order to develop a new type of rechargeable MnO_2 material, attempts have been made to introduce dopant ions into manganese oxide material [27–34] using various methods. Various foreign ions were introduced, but only Bi and Pb, as found by Wroblowa and coworkers [29–34], seem to have high effectiveness in making MnO_2 rechargeable. Two kinds of methods were used to introduce the dopants, Bi or Pb, into MnO_2; one was a coprecipitation method leading to a so-called 'chemically modified' electrode; the other was a procedure of mechanically mixing Bi_2O_3 or PbO with γ-MnO_2, leading to a 'physically modified' electrode.

Both the chemically modified MnO_2, referred to here as CM MnO_2 and the physically modified MnO_2, referred to as PM MnO_2, have shown rechargeability at the two-electron level. The effect of added Bi(III) was considered in the light of the previously treated mechanisms of reduction/reoxidation; since the reduction involves the insertion of protons and electrons, the cation radii consequently increase resulting in major restructuring of the lattice. The effect of added Bi(III) may be to stabilize the lattice towards such dimensional changes by modifying the 'open structure' configuration [29–31], but it is difficult to account, on such a model, for the fact that the influence of Bi(III) is already observable at low levels of 1–2 mol % in the MnO_2 material. Secondly, the CM MnO_2 becomes rechargeable over the two-electron reaction. Considering that the Mn(III) intermediate is soluble, it is hard to understand the significance of the supposed 'open structure' effect. However, the rechargeability of the CM MnO_2 electrodes was dramatically reduced when Wroblowa and coworkers [29–33] attempted to develop an actual MnO_2–Zn rechargeable battery. The loss of rechargeability of CM MnO_2

electrode was found to arise on account of dissolution of zinc leading to a high concentration of zincate ion which interferes with the rechargeability of $Mn(OH)_2$ due to irreversible formation of zinc bernessite. Several attempts in those works of Wroblowa at the Ford Motor Company, including applying a number of organic materials to depress the solubility of zincate ions, and using ion-selective membranes to block zincate ion transfer to the cathode, have been made. However, since the mechanisms of reduction and oxidation of CM MnO_2 were not completely characterized by those authors, the problems could not be fully solved in their work at that time.

In the present work, both classical electroanalytical and *in-situ* u.v.-visible spectro-electrochemistry methods have been used in studying Ford's CM MnO_2 [32, 33] in order to elucidate further the role and behaviour of the soluble intermediate involved in multiple cycling. The purpose of the spectroelectrochemical experiments was to examine if there are significant differences in the production of soluble Mn(III) species from discharge and recharge of CM MnO_2 in comparison with blank MnO_2 (no Bi) or γ-MnO_2, and hence obtain an indication of whether the role of the intermediate stage is changed by the doping of MnO_2 by Bi(III).

In complementary work on comparison of the kinetics of charging and discharging of CM MnO_2 with that at γ-MnO_2, we have shown elsewhere [35] that the CM material can sustain higher current densities (per gram of active material), both on charge and discharge, than the γ-MnO_2 material, at a well defined discharge potential plateau (shown in Fig. 4, curve b; see later).

2. Experimental details

2.1. *Material*

CM MnO_2 was prepared according to Ford's patent [32, 33]; the Mn/Bi ratio was 8.75/1 (original ratio of $Mn(NO_3)_2$ to $Bi(NO_3)_3$). 'Blank' MnO_2 (no bismuth incorporated) was used as a comparative or reference system; the preparation procedure was the same as that for CM MnO_2 but without addition of the bismuth component. γ-MnO_2 was the international common sample, I.C. No. 2.

2.2. *Design of cell and electrode holder*

The cell was a three-compartment, specially constructed, airtight Teflon cell enabling strong KOH electrolyte to be used without the problems arising with a glass cell. A special Teflon electrode holder was used to accommodate and mount a compressed MnO_2 + C electrode matrix by means of a screw-fitting plug. Another cell was of a flat cell design, made of Perspex, which could accommodate a special rolled MnO_2/graphite/Teflon-bonded electrode.

2.3. *Electrolyte, reference and counter electrodes*

9 M aq. KOH solutions were used as electrolyte in all experiments at a temperature of 298 K. Solutions were outgassed from oxygen by bubbling nitrogen for 1 h before the experiments were begun. All potentials reported, unless otherwise specified, are referred to the Hg/HgO reference electrode which was immersed in KOH of the same concentration as the experimental electrolyte. A platinum-mesh counter electrode was used.

2.4. *Construction of MnO_2 powder electrode*

Three kinds of MnO_2 powder electrode material were used in the experiments in order to examine the relation between electrode structure and loss of rechargeability: (i) a non-pressed electrode which was mounted as a hard paste in contact with and between two pieces of platinum mesh used as the current collector; (ii) an electrode which was compressed at a pressure of about 7.5 ton cm^{-2} into pellets and mounted between two platinum-mesh sheets; (iii) a specially rolled film: 5 ~ 10 wt% (dry material) of Teflon suspension was used as a binder, then the active material (MnO_2/Teflon/graphite) was rolled to form a film which was then mounted between the platinum-mesh sheets or compressed on a nickel-mesh to form the positive electrode.

Unless otherwise mentioned, three types of working electrodes were, respectively, made of a mixture of the three kinds of MnO_2 milled with Lonza graphite in 1 : 10 ratio plus 5% (by weight) of acetylene black (Shawinigan Chemical Company).

2.5. *Cyclic voltammetry*

The electrodes used in the CV experiments were of the nonpressed type. After they were mounted into the holder, the electrodes were immersed in aq. 9M KOH solution for 1–2 h to ensure that the whole electrode became wetted, and then subjected to a linear potential sweep (0.5 mV s^{-1}). Two procedures were used in these tests: one involved repetitive cycling, the other potential holding where the cathodic sweep was stopped at various potentials along the sweep range for a controlled period of time, then the direction of potential sweep was reversed to that for anodic polarization.

2.6. *Constant discharge (galvanostatic) experiments*

Here the MnO_2 electrodes were discharged and recharged in aq. 9 M KOH solution at a certain constant current density at 298 K ± 1 K.

2.7. *Constant-current discharge with the stationary detector electrode*

The electrodes used in these experiments were of the compressed type. The electrodes were mounted between two platinum-mesh supports which acted as current collectors. The MnO_2 working electrode and the platinum detecting electrode were separated by a

thin perforated Teflon separator. Here, the soluble manganese species produced during discharge of the CM MnO_2 electrode was detected by its further reduction or its reoxidation at the platinum detector electrode after if had diffused through the separator. Both the working and detector electrodes were encapsulated in a separator membrane and hand-pressed into the holder by screwing in a Teflon plug. If any soluble species were produced during discharge of the MnO_2 electrode, they could diffuse easily to the detector electrode where, at the potential of the latter, they would become reoxidized. Therefore any anodic current appearing additionally to the background current (due to oxygen reduction) indicated the formation of the soluble Mn(III) species.

The potential of the detector electrode was held at -50 mV while the working electrode was being discharged. Potential control of both the generator electrode (the MnO_2 cathode) and the detector was achieved by means of a Pine Instrument Co. bipotentiostat, as used with rotating ring-disc electrodes (Section 2.8).

2.8. *Rotating ring disc electrode (RRDE) experiments*

The MnO_2 electrodes used in the RRDE experiments had to be specially designed. A carbon/Teflon matrix, rolled as a film, was first fitted as a conducting disc into a circular depression (0.5 mm deep) of a rotating gold ring-disc system. The CM MnO_2 powder was then coated on to this matrix by pressure. The potential of the gold ring was controlled at -0.1 V.

2.9. *In situ u.v.-visible spectro-electrochemistry*

An important series of experiments was conducted spectro-electrochemically to detect, *in situ*, the formation of soluble Mn(III) species from CM or regular γ-MnO_2 under discharge or subsequent recharge. A special small plate-geometry cell, sealed to a 1 cm u.v. spectrometer cuvette, was constructed so that the formation of electrogenerated soluble species could be directly followed spectrophotometrically. Generation or removal of Mn(III) species on both discharge and recharge could be followed as a function of time and electrode potential as the soluble species diffused out from the MnO_2 electrode or was redeposited in it. The spectrophotometer also provided a wavelength scan readout of the optical absorption which could be followed quite quickly at various times and after various periods of discharge or recharge. The kinetics of the processes involved in these experiments were determined by diffusion out of or back into the MnO_2/C cathode material matrix, aided by stirring of the solution with oxygen-free nitrogen.

The *in situ* u.v.-visible spectrochemistry cell used in these experiments is shown in Fig. 1 and consisted of two parts: the upper was made of Pyrex and the lower, which was located in the optical pathway of the spectrophotometer, was made of quartz (a commercial 1 cm u.v. cuvette). The two parts were sealed together. Hg/HgO was used as the reference and platinum wire as the counter electrode. The low-valent manganese species of interest in the present work are formed during the reduction of MnO_2 or in reoxidation of reduced Mn species but oxygen is unavoidably generated at the counter electrode. Since these Mn species are easily oxidized by oxygen in alkaline solution, an ionically conducting membrane was used to block the diffusion of this oxygen into the main compartment of the cell containing the MnO_2 cathode. During anodic recharge of the MnO_2 electrode, hydrogen evolved at the platinum electrode was also blocked by the membrane.

A moveable fine Teflon tube, through which nitrogen could be passed to the bottom of the quartz cell for bubbling, could be introduced through the top of the cell. There are two purposes of bubbling nitrogen during the charge and discharge process: one is to initially expel dissolved oxygen to avoid oxidation of the Mn(III) species; the other is to stir the solution to ensure that the soluble species formed from the MnO_2 electrode, located in the upper section of the cell, can be transported to the lower optical curvette immediately. The Teflon tube was moved out of the light path when optical measurements were performed, with the cell remaining free of oxygen.

2.10. *Instrumental*

Principal instruments used in the work were a PARC 273 potentiostat controlled by means of M270 software, a PINE AFRDE4 bipotentiostat and a PINE AFASR Rotator which were used in experiments conducted at a rotating ring-disc electrode. Constant current discharge experiments were also carried out with a stationary detector electrode. The u.v.–visible spectrophotometer used was a Perkin–Elmer Lambda 3B instrument. The output u.v.-visible data were recorded and accumulated by means of a Nicolet 310 digital oscilloscope. The atomic absorption spectrophotometer used was the Varian AA-1475 series. The digitized data were processed by a PC by means of appropriate software.

3. Results and discussion

3.1. *Cyclic voltammetry*

Figure 2 shows the 2nd cycle of cyclic voltammetry (CV) at the MnO_2 and Fig. 3 the cathodic capacity changes against the number of cycles for CM MnO_2, γ-MnO_2 and blank MnO_2. The significant rechargeability achieved with the CM material can be clearly observed, in agreement with Wroblowa's previous work [29, 31]. The difference of the first cycle response from those of subsequent ones originates partly from the unavoidable initial presence of adsorbed oxygen in the porous, high-area electrode.

The two cathodic peaks observed in the current-potential diagram (Fig. 2) may be associated with the

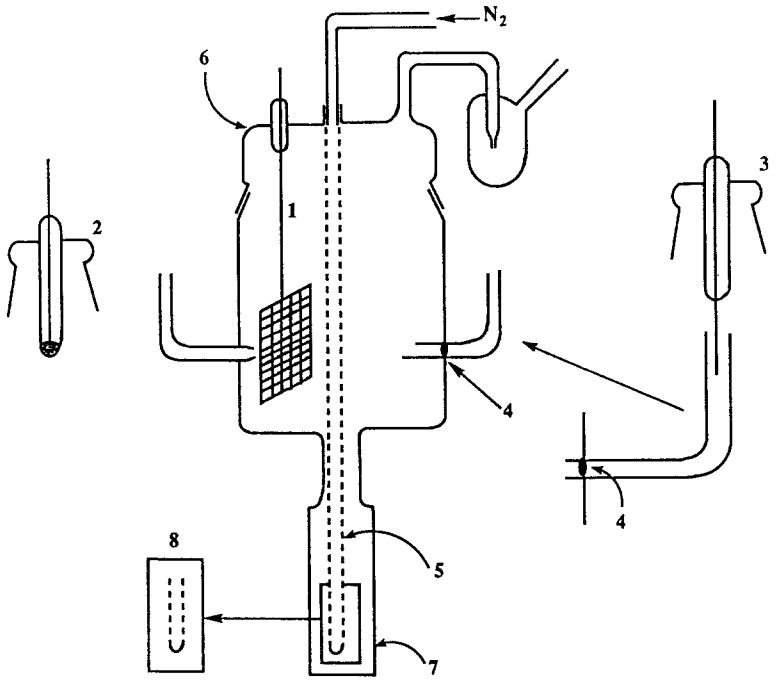

Fig. 1. Optical-electrochemistry cell. (1) MnO_2 working electrode; (2) Hg/HgO reference electrode; (3) Pt wire counter electrode; (4) membrane; (5) moveable fine Teflon tube for bubbling of nitrogen; (6) Pyrex top; (7) quartz cuvette (1 cm); (8) perforated bottom of Teflon tube.

two-stage reduction involving the first and second electron. (Other small peaks due to bismuth reduction or reoxidation can also be observed, depending on the potential range in the CV). Sometimes, however, the two (Mn) peaks become combined into one, depending on the Bi/Mn ratio (high Bi/Mn material shows two peaks), the type of electrolyte (two peaks are better resolved in NaOH than in KOH electrolyte), the surface area of carbon (two peaks are better resolved when the MnO_2 is mixed with high-area carbon) and the sweep-rate (at a sufficiently low sweep-rate, the two peaks merge into a single one [35]). These effects may arise because of the different conductivity of both electrolyte and electrode which can influence the further reduction of soluble Mn(III) in solution or that adsorbed on the porous electrode structure, as will be discussed later.

3.2. *Constant-current discharge*

Figure 4 shows a comparison of the constant current discharge characteristic of CM MnO_2 (curve b) with that of γ-MnO_2 (curve a). Two regions can be distinguished in curve a corresponding to the homogenous and heterogenous processes as proposed by Kozawa [3, 4] but in curve b there is only one flat region and a small flat tail at its end, corresponding approximately to 10% of the flat region capacity, due in part to

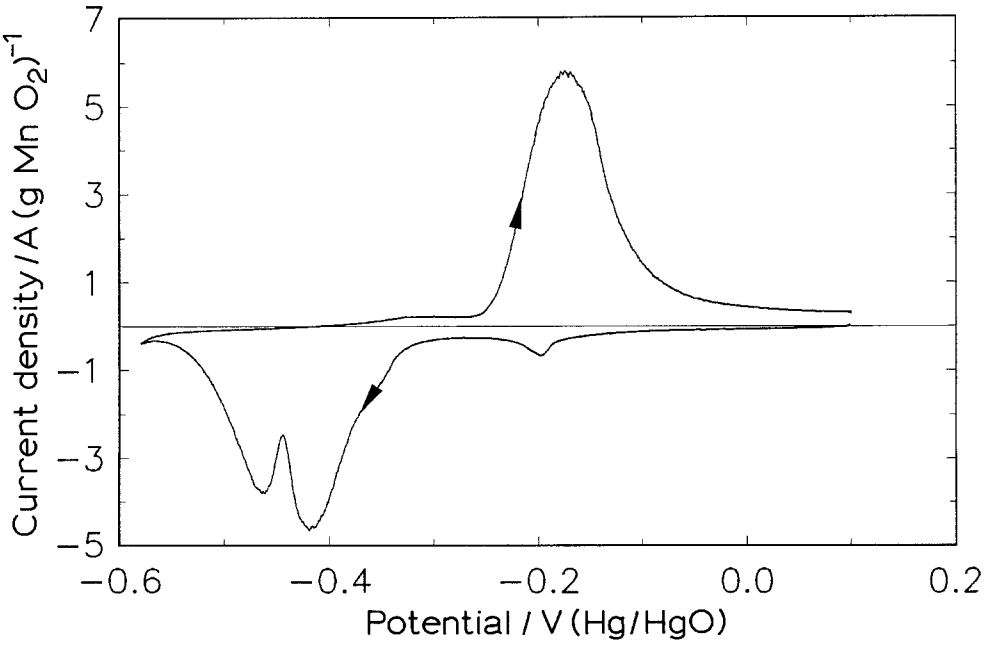

Fig. 2. Cyclic voltammetry of CM MnO_2 in 9 M aq. KOH solution at 298 K. Sweep rate: 0.5 mV s^{-1}.

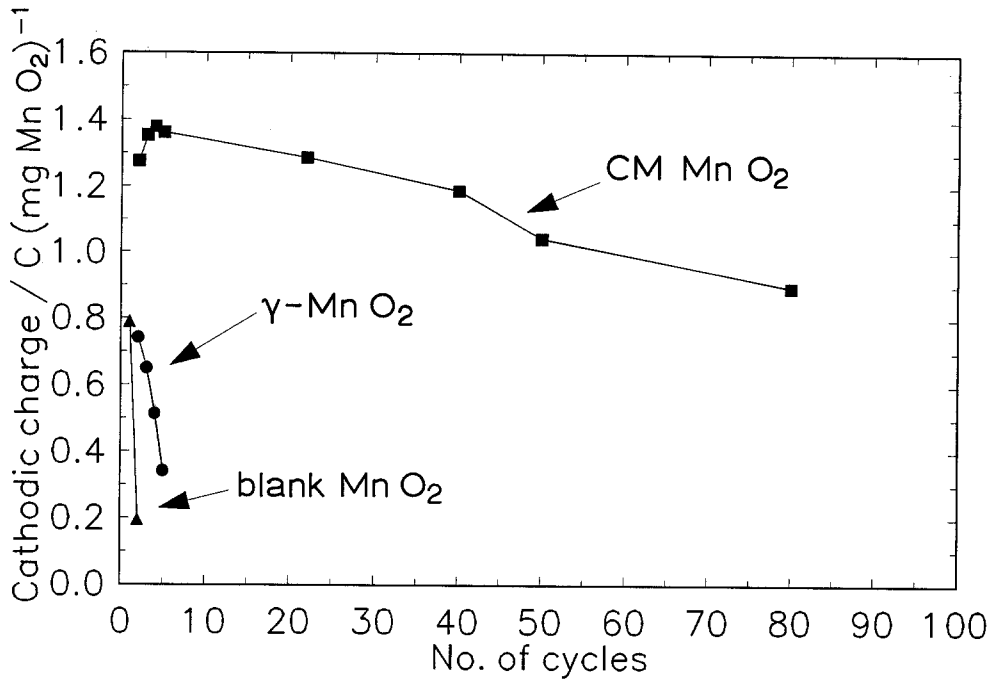

Fig. 3. Comparison between the cycle lives of CM MnO_2. γ-MnO_2 and blank MnO_2. The number of charge/recharge cycles represents the number of cycles covered in cyclic voltammetry. Sweep rate: $0.5\,mV\,s^{-1}$.

Bi_2O_3 reduction. Since almost no change of potential arises on discharge, the first step of reduction of CM MnO_2 can be considered as an heterogenous process, based on Vetter's theory [10]. Theoretically, based on the Nernst equation, when one solid phase is electrochemically reduced to another solid phase at unit activity or to a saturated state of dissolved species (since the ratio of activities of higher to lower oxidation-state material remains constant during the discharge process), the o.c.p. (open circuit potential) of the system should remain constant as long as both phases coexist. Although such criteria can only really be used for equilibrium conditions, in the present experiments, the discharge and recharge currents were relatively low, so the restricting conditions can be assumed to be fulfilled. Therefore the Mn(III), which is the first product of reduction of CM MnO_2, can be either in the solid state or dissolved in a saturated state (see below), or both.

In other experiments [35], it was shown that once the potential of the 'flat region' of the discharge curve had been reached around 10% or less of discharge capacity, it remains almost *independent* of cathodic current density up to the 6C rate, i.e. polarization effects in that state remain small in the continuing discharge of the CM material (cf. Fig. 4, curve b).

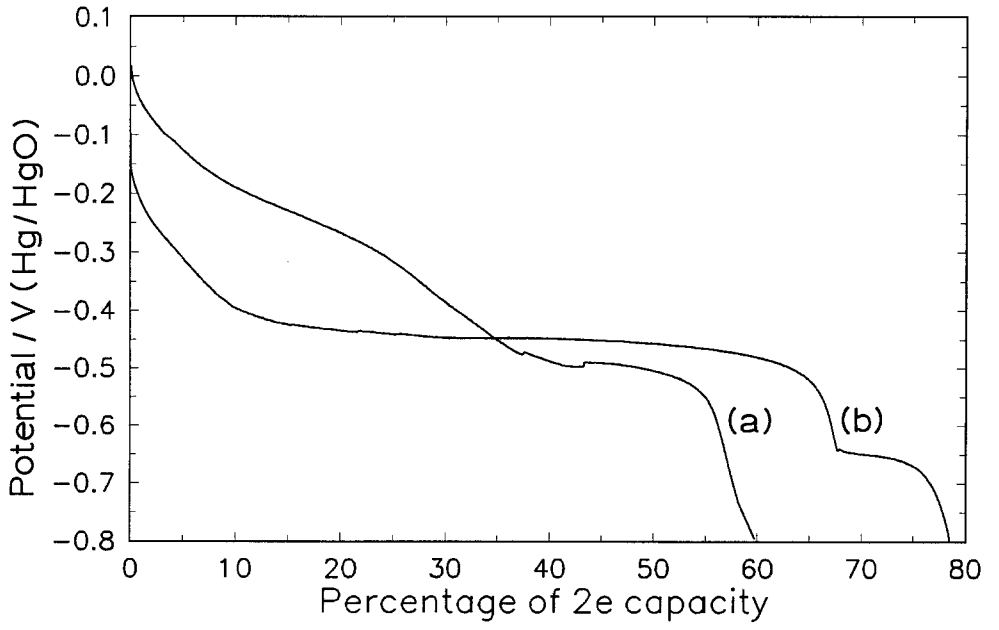

Fig. 4. Constant current discharge of CM MnO_2 (curve b) and of γ-MnO_2 (curve a). Current density $0.2\,A\,g^{-1}$.

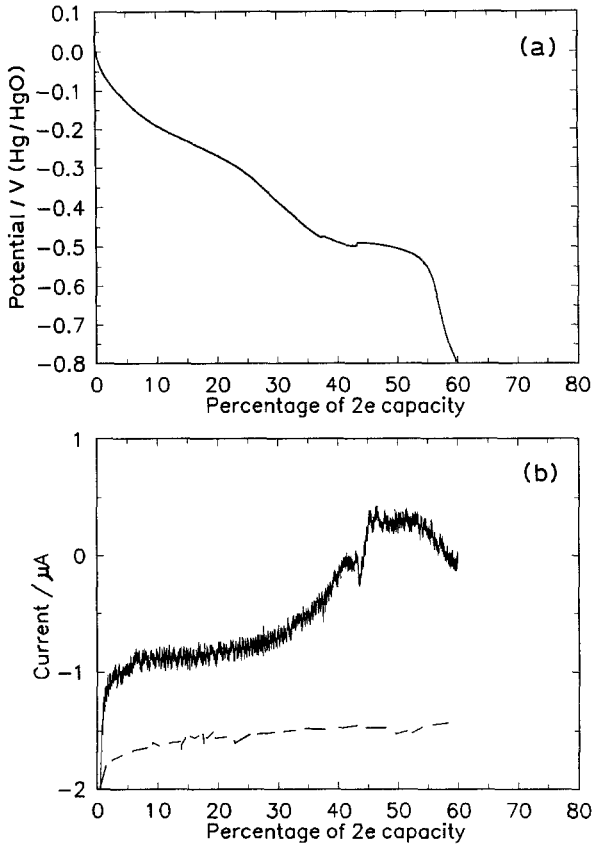

Fig. 5. Constant current discharge of a γ-MnO_2 electrode showing the platinum detector electrode response. (a) Constant-current discharge of γ-MnO_2; I density = $0.2\,A\,g^{-1}$. (b) Response on the platinum detector electrode. Potential: -50 mV against Hg/HgO. Dashed line represents background current.

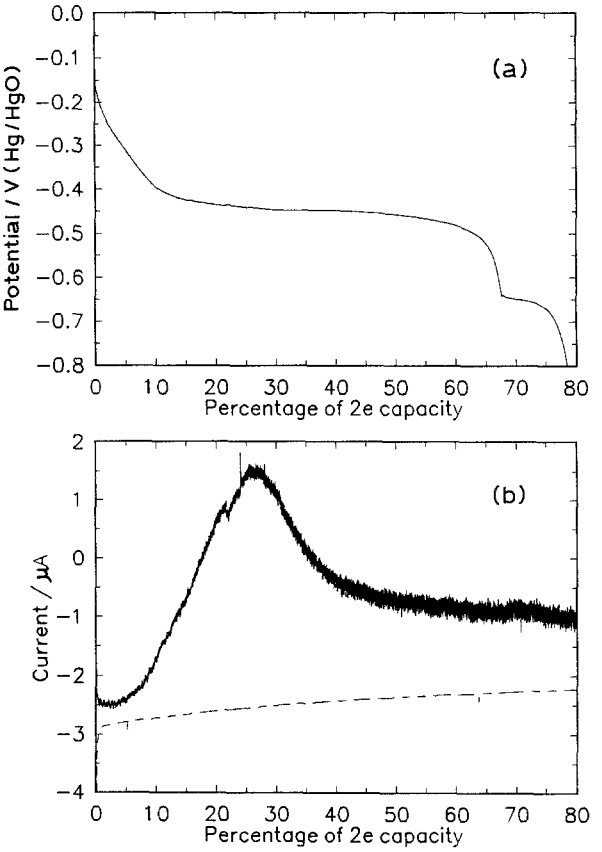

Fig. 6. Constant current discharge of the CM MnO_2 electrode with the platinum detector/electrode. (a) Constant current discharge of the CM MnO_2; current density = $0.2\,A\,g^{-1}$. (b) Response on the platinum detector electrode. Potential: -50 mV against Hg/HgO. Dashed line represents background current.

3.3. *Detection of Mn(III) intermediate(s) in solution with the detector electrode*

Figures 5 and 6 show the results of constant current discharge experiments with a stationary detector electrode, the potential of which was held at -50 mV against Hg/HgO. The electrodes were γ-MnO_2 (Fig. 5) and CM MnO_2 (Fig. 6), respectively. The upper curves in Figs 5 and 6 shows the results of constant current discharge and the lower ones the current response at the detector electrode. The dashed lines in Figs 5(b) and 6(b) show the background reduction current of residual oxygen which was either in the solution or adsorbed in the porous MnO_2 electrode, and can also initially diffuse to the detector electrode. The positive oxidation current signal at the detector electrode would, of course, be added algebraically to the negative background reduction current for oxygen, referred to above.

In the first step of γ-MnO_2 discharge, which is proved to be homogeneous [8, 14], there is already a small but significant detector response due to dissolved species, as expected; however, in the second step which begins at approximately 30% of two-electron (2e) capacity, a significant increase of the signal arises which must result from generation of soluble species as seen in Fig. 5(b). The soluble species may be $Mn(OH)_6^{3-}$ and it is evident that such species are generated from γ-MnO_2 but to a smaller extent than from CM MnO_2, referred to below.

These results are consistent with Kozawa's proposal [5] of a two-step reduction mechanism. In the case of CM MnO_2, Fig. 6 shows that soluble species are formed as soon as the discharge process begins (also refer to Fig. 13b). The discharge processes on the working and detector electrodes can be summarized as follows (see Fig. 6):

(i) In the range of 0–5% of 2-e capacity, the 'soluble' Mn(III) species, we suggest, remain adsorbed on the distributed surface of the porous electrode structure. Beyond about 5% of extent of discharge, adsorbed Mn(III) species will increase their occupancy of the C surface and the activity of soluble Mn(III) will tend to increase in the pores until the electrolyte there becomes saturated. So, during this step, the potential of the MnO_2 becomes reduced and no significant signal arises at the detecting electrode. Thus, in the initial stage of discharge, a mixed heterogeneous and homogeneous mechanism would apply.

(ii) The porous powder electrode becomes saturated by soluble Mn(III) species and the excess Mn(III) begins to diffuse out to the bulk solution, and can then provide a response signal at the detector platinum electrode. The potential of the MnO_2 electrode remains relatively stable (Fig. 6a) and the current at the detector electrode continues to increase (Fig. 6b).

(iii) The Mn(III) species then begins to be further

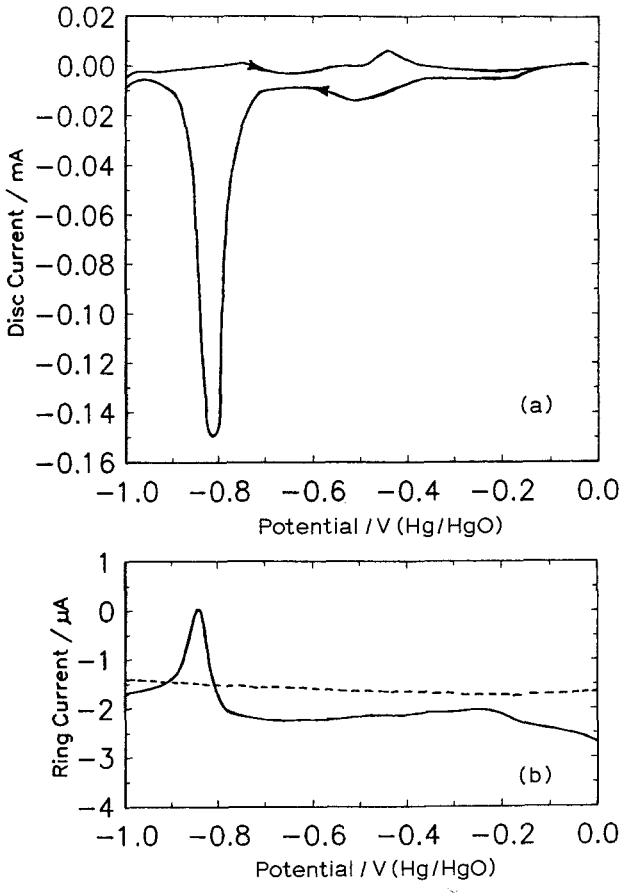

Fig. 7. (a) CV profile of a CM MnO_2/acetylene black RRDE electrode, on the MnO_2 disc, at a sweep-rate of 0.5 mV s^{-1} and rotation rate of 2000 r.p.m. (b) dependence of corresponding ring (Au) current on the electrode potential of the disc. The gold ring potential was held at −0.1 V against Hg/HgO. Dashed line shows background current.

reduced on the porous electrode, forming $Mn(OH)_2$ which begins to precipitate out of solution onto the substrate. In this step, the reductions of MnO_2 to Mn(III) and Mn(III) to $Mn(OH)_2$ are probably taking place simultaneously.

Another point must be mentioned about the above experiments: considering the time scale (3 h) needed to discharge 100% of the theoretical two-electron capacity and the tightly constructed electrode, the experiments can be treated virtually as providing *in situ* detection of soluble Mn species, i.e. relatively no significant delay in the detector electrode response is seen. In other words, almost as soon as soluble low-valence Mn species are formed, a response is seen at the detector electrode.

3.4. *Detection of Mn(III) intermediate(s) at the RRDE electrode*

Figure 7 shows the results at a ring-disc electrode rotated at 2000 r.p.m. in an experiment carried out with continuous bubbling of nitrogen. Figure 7a shows the signal on the MnO_2 disc electrode while Fig. 7b that on the gold-ring held at −0.1 V. When the electrode is rotated, the soluble low-valence species formed at the disc are spun out to the ring and reoxidized there. Because the MnO_2 powder constituting the disc had to be hand-pressed on to the surface of the matrix, the contact between the MnO_2 particles and the carbon matrix could hardly be the same from one electode to another, that is the contact resistance of the electrodes was unavoidably not uniform from one electrode to another, so the cathodic polarization at each of the electrodes was not identical and some variation of polarization of the electrode was unavoidable. However, considering the time (25 min) which it took for the potential to change from the initial value (0.0 V) to the potential of appearance of the cathodic peak (~ -0.75 V), the MnO_2 particles can be treated as being firmly coated on the surface of the matrix otherwise they would have been thrown out from the disc during the above period.

Figure 8 shows the change of ratio of the anodic reoxidation charge to the cathodic reduction charge at the MnO_2 disc electrode, with electrode rotation rate.

Two aspects are to be noted here: first, a significant oxidation peak arises at the ring (Fig. 7b) corresponding to the peak for reduction of MnO_2 in the disc electrode (Fig. 7a) when the latter was rotated. This result supports the previous *in situ* observation of formation of soluble Mn species during discharge. Secondly, the ratio of the reoxidation charge to the reduction charge at the MnO_2 disc electrode decreases with increase of rotation rate. When the rotation rate is high enough, *no* re-oxidation signal is detectable (Fig. 8); this shows that the CM MnO_2, like γ-MnO_2 [12], can be fully reduced to soluble species.

Because the MnO_2 has to be accommodated in the porous carbon surface, the soluble species tend to stay there, but if the rotation rate is high enough, the soluble species can be spun away to bulk solution soon after they are generated by reduction of MnO_2. If the electrode is, however, kept stationary, most of soluble species can, of course, remain adsorbed or occluded in the vicinity of the electrode surface except for some small fraction that still diffuses into the bulk solution. These adsorbed and absorbed ions could be further reduced to $Mn(OH)_2$ precipitated onto the porous electrode and then reoxidized to MnO_2 on recharge.

3.5. *Potential holding experiments*

In irreversible processes studied by means of linear-sweep voltammetry, complementary kinetic information can be obtained by arresting the sweep at some defined potential in the swept range and then following the time dependence of the current.

Figure 9 shows such behaviour in a potential holding experiment: after a 1st cycle to reduce adsorbed oxygen, the potential sweep was stopped at various values along the swept potential range (Fig. 9a) and held until the cathodic current reached a stable value close to zero (except for curve 3); then the direction of potential sweep was reversed to that of anodic polarization. For curve 3, where the potential was held at −0.43 V (which is the potential corresponding to the flat region in the galvanostatic diagram, see Fig. 4 curve 2), the cathodic current kept decreasing until it reached point ✡ (where the current was not zero)

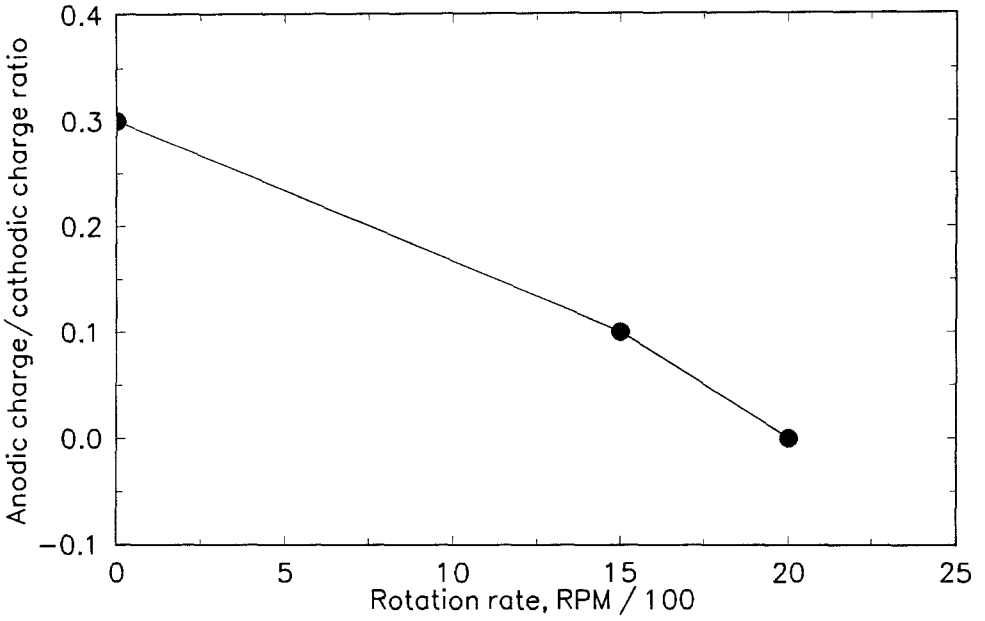

Fig. 8. The change of the ratio of anodic to cathodic charge at a CM MnO_2/acetylene black matrix electrode with rotation rate.

whereupon it began to increase. Figure 9c and d show the time dependence of the cathodic current during potential holding for curves 3 and 4, respectively.

It is interesting to point out, from the results in Fig. 9, that the mechanisms of the reduction of CM MnO_2 and γ-MnO_2 are dramatically different: the full 2e capacity of CM MnO_2 can be discharged at about -0.43 V and can then be recharged, while γ-MnO_2 can only give 1e capacity if discharged in the range of $-0.4 \sim -0.6$ V, and cannot be recharged, unless it is further reduced to $Mn(OH)_2$ at about -1.0 V [14]. This unique feature gives CM MnO_2 electrodes twice the usable energy density in comparison with regular γ-MnO_2 electrodes [35].

It can be observed from Fig. 9 that the highest anodic peak arises only in curves 4 and 5. In addition, there is a new peak in the potential range $-0.3 \sim -0.25$ V, which increases from curve 1 to 2 to 3. The anodic peak in curve 4 of Fig. 9a and b can be assumed to be associated with the process $Mn(OH)_2 \longrightarrow [Mn(III)] \longrightarrow MnO_2$. In curve 3, the anodic peak may be due to the reoxidation of soluble Mn(III) species on the surface of the porous electrode. Since, in curve 3, the cathodic current has not reached zero when the current began to increase, the sudden increase of current in that curve suggests that the second electron reduction can take place, coupled with the first electron reduction and at the *same* potential when the first electron reduction has proceeded to a certain stage. In Fig. 9c, the current which decreases in the first 8 min results from the reaction of $MnO_2 \longrightarrow$ Mn(III) and the sudden increase of the current results from another reaction which could be assumed to be Mn(III) $\longrightarrow$ $Mn(OH)_2$ (Fig. 9d).

Furthermore, the soluble Mn(III) species itself can be electrochemically reoxidized to MnO_2 which can then be rereduced and reoxidized again and again, while the Mn(III) in the products of γ-MnO_2 reduction cannot be reoxidised electrochemically [14, 35].

3.6. *Detection of Mn(III) species by means of spectroelectrochemistry*

The cell and procedure described earlier were employed. Mn(III) species were generated on discharge or recharge of MnO_2 cathode preparations.

In our previous work, brown coloured soluble species were a product of the cathodic process. The species and their dissolution into bulk solution are quite critical in the mechanism of discharge/recharge of the MnO_2 material.

The solid line (Fig. 10) shows a typical optical absorption spectrum of soluble, low-valent Mn(III) species formed in the process of discharge of MnO_2. Hexacoordinated trivalent Mn complexes generally exhibit a single band in the 470 nm region [36, 37]. Direct measurement of the spectrum of trivalent Mn in concentrated KOH solution confirmed this result in showing a single band in the visible region with a peak at 465 nm, which may therefore tentatively be ascribed to the ion $[Mn(OH)_6]^{3-}$ [12]. Quite positively, the low oxidation state Mn species could be identified as hydrous Mn(III) ion from the spectrum. Such trivalent Mn species were found to be formed not only in the discharge process, but also in recharge. In Fig. 10 are compared the absorption spectra of the species formed in discharge (solid line) with those in the recharge process (dashed line). It is seen that the shapes of the curves and the locations of maximum absorption (465 nm) are exactly the same. Hence the same Mn ion species are generated both in the cathodic and the anodic processes.

Considering the rechargeability of the material, it might be concluded logically, that the mechanism of CM MnO_2 on discharge should be similar to that on recharge; at least both processes evidently involve the same intermediate(s). As was described earlier, Mn(III) species were detected already at an early stage of discharge (unlike the behaviour of γ-MnO_2).

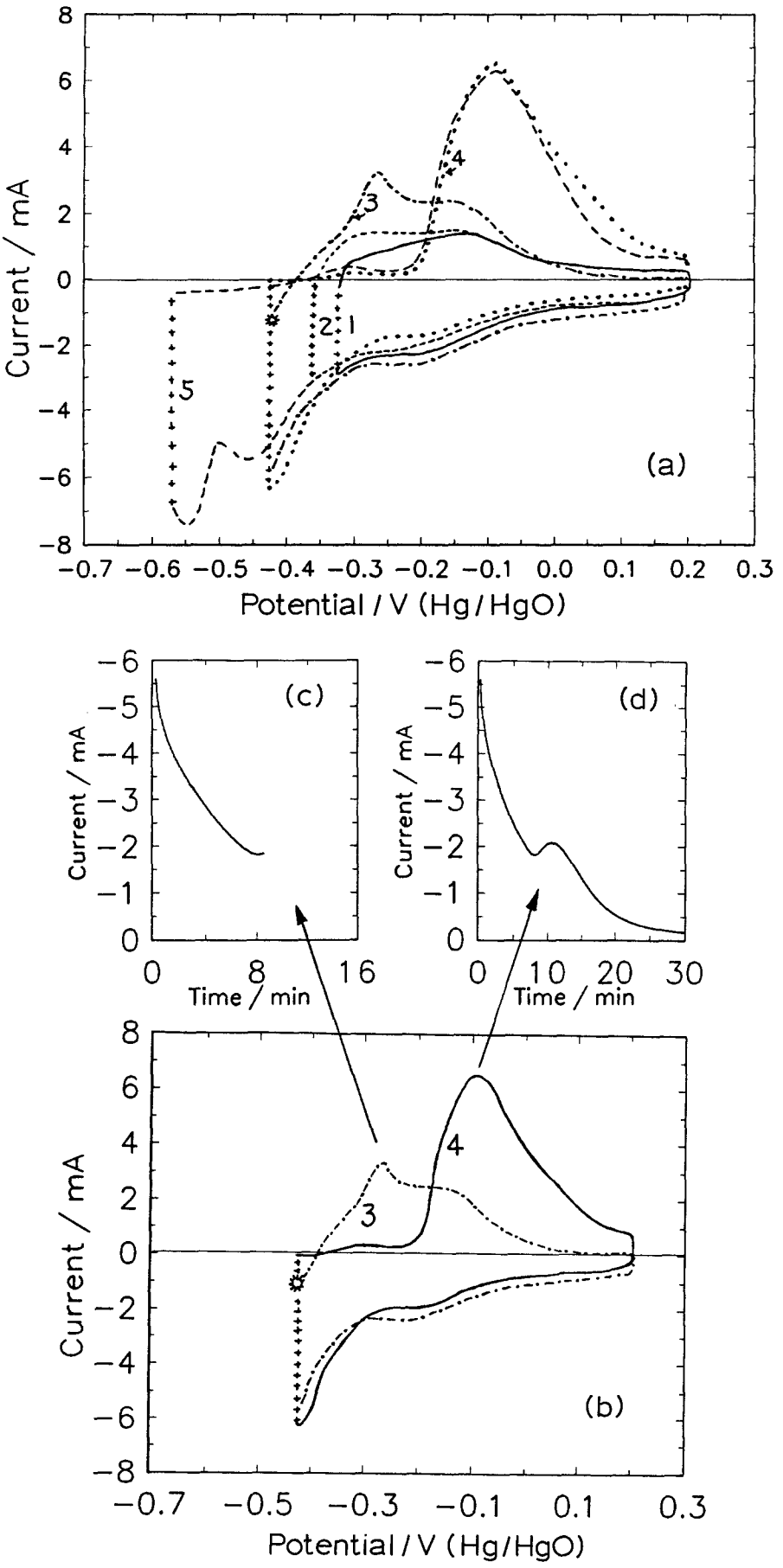

Fig. 9. Current variations in CV experiments (0.5 mV s^{-1}, started at 0.2 V and swept in the cathodic direction) on CM MnO_2 with potential holding. (a) Potentials held at (1) −0.32; (2) −0.37; (3) and (4) −0.43 and (5) −0.57 V against Hg/HgO until currents approached zero (except curve 3, see following). (b) Potential held at −0.43 V against Hg/HgO (curves 3 and 4). The time dependence of the current during holding is shown in Figs. 9c and 9d. Curves 3 and 4 are the same as those in (a). (c) and (d) show time dependence of the cathodic current during the potential holding experiments corresponding to curves 3 and 4, respectively.

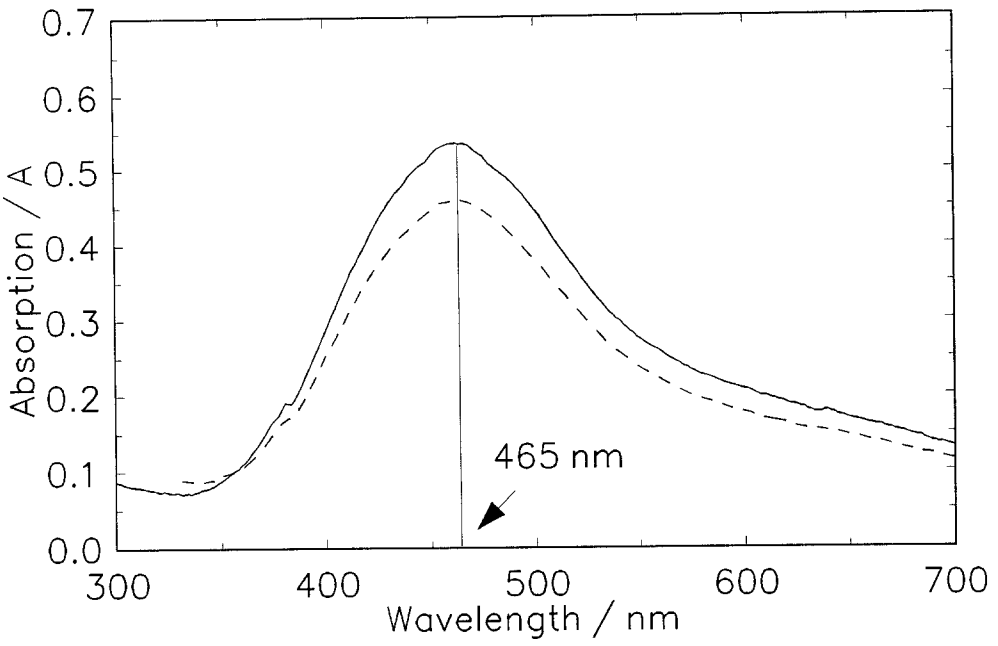

Fig. 10. U.v.-visible spectra of soluble Mn(III) species; solid line for 37% discharge; dashed line for 37% on recharge of 2e capacity of a CM MnO_2 electrode.

Figures 11 and 12 show the spectra observed at different percentages of discharge and recharge, respectively. The upper diagram (a) in Fig. 13 shows the results of constant current discharge (solid line) and recharge (dashed line) at the same polarization current density value as in the optical experiments; the lower one shows the maximum absorption at different levels of capacity in both discharge and recharge directions. The arrows indicate the directions of polarization.

From Fig. 11, it is seen that, before discharge (0%), there is no significant absorption over the whole wavelength range. When, however, discharge is started, absorption in the visible can be observed and continues to increase. At the stage of 25% of 2e capacity discharge, the absorption density (Fig. 13b) is almost 80% of its highest value but 25% consumption of capacity is still the early stage in the overall discharge process (see Fig. 13a). The concentration of $[Mn(OH)_6]^{3-}$ (corresponding to the absorption density, Fig. 13b) increased in the early stage of discharge but the concentration began to decrease in the range of 40 to 50% of two-electron capacity with no significant decrease of discharge potential (Fig. 13a). From Fig. 12, it is seen that, similar to the cathodic process, in the early stage of recharge, the concentration of $[Mn(OH)_6]^{3-}$ increased with polarization time (80% $\longrightarrow$ 76% $\longrightarrow$ 50% of discharge capacity), and then the concentration began to decrease in the range of 50 to 40%. As in the case of discharge, the recharge potential (Fig. 13a) of the MnO_2 electrode

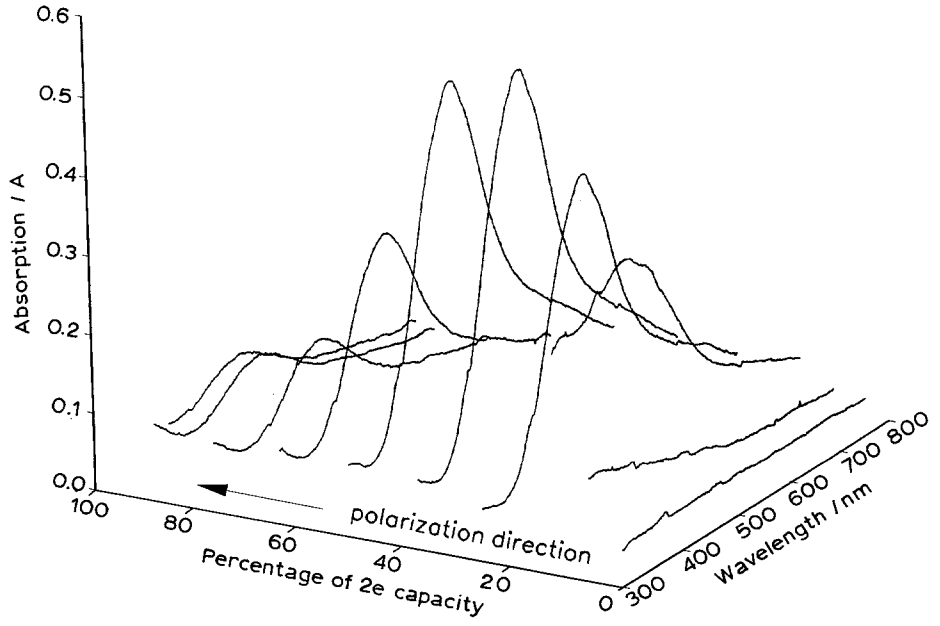

Fig. 11. The change of optical absorption spectrum of Mn(III) species with percentage discharge in the discharge process at a CM MnO_2/Lonza graphite mixture (1 : 4).

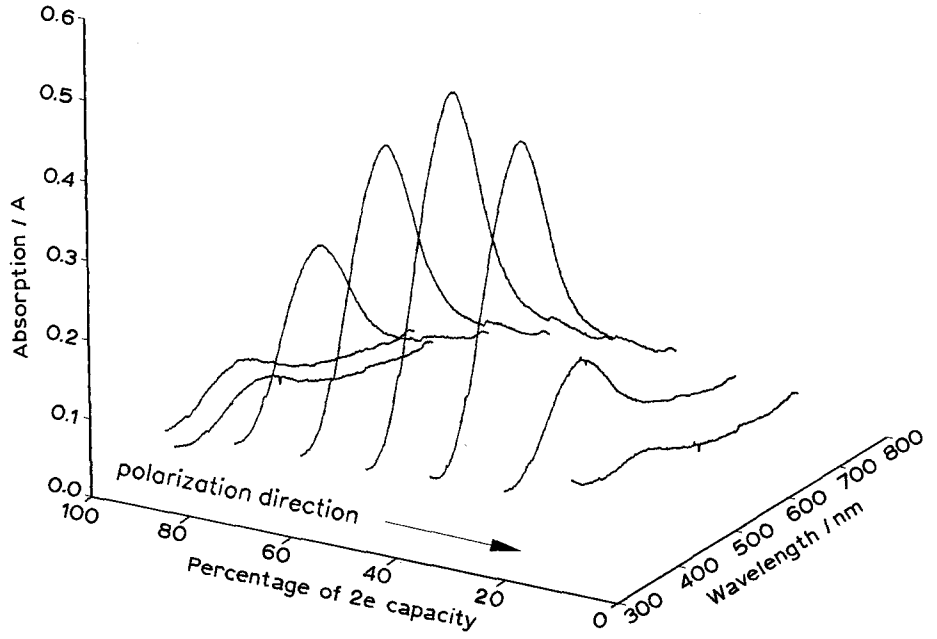

Fig. 12. Change of absorption spectrum of Mn(III) species with percentage discharge in the recharge process at a CM MnO_2/Lonza graphite mixture (1 : 4).

also did not importantly change when the concentration of $[Mn(OH)_6]^{3-}$ began to decrease (see Fig. 13b). Comparing the density of the maximum absorption in both the discharge and recharge process (Fig. 13b), it can be seen that the densities of the maximum absorption in both cases are almost the same, i.e. the highest concentrations of soluble $[Mn(OH)_6]^{3-}$ ions in solution, formed in both the cathodic and anodic processes, are almost the same. It must be emphasized that there was a relatively large volume of free electrolyte in the optical cell.

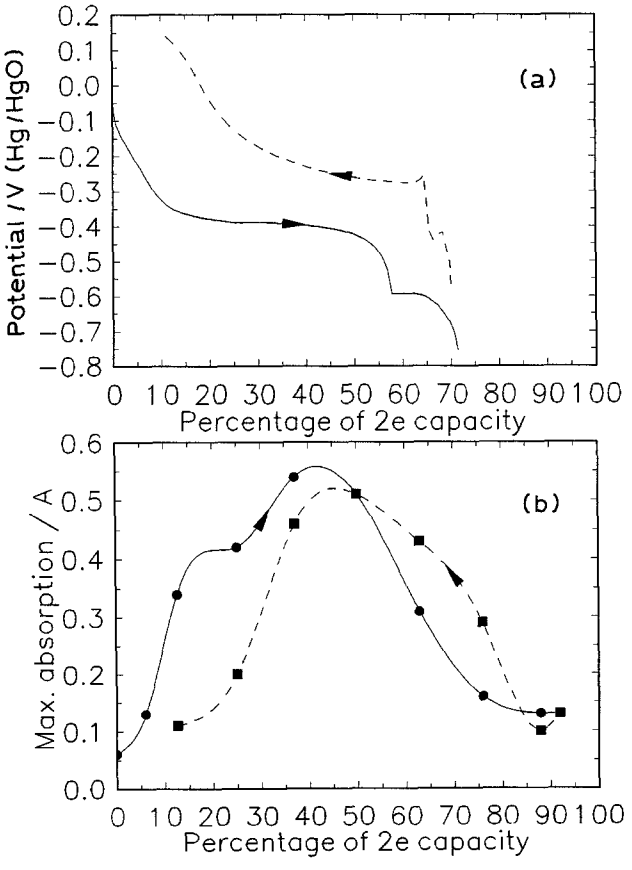

Fig. 13. Comparison of constant current discharge and recharge curves (a) with maximum absorption at various stages of discharge and recharge (b). CM MnO_2/Lonza graphite = 1 : 4; current density = $0.16\,A\,g^{-1}$; solid line: discharge; dashed line: recharge.

From Fig. 13b, firstly on both the left hand and right hand sides of the diagram, the concentrations of $[Mn(OH)_6]^{3-}$ (absorption) at the beginning of discharge (0 ~ 5%) are similar to those at the end of discharge. Secondly, for both discharge and recharge, the concentration of $[Mn(OH)_6]^{3-}$ changed with percentage in an inverted V-shape and the changes of the concentration switched from increasing to decreasing directions, both in the range of 40 to 50% discharge.

The $[Mn(OH)_6]^{3-}$ is not a stable ion; it can be oxidized to MnO_2 by oxidizing agents such as oxygen. It can also *disproportionate* in the following way, represented in terms of the simple cations:

$$2Mn^{3+} + 2H_2O \rightleftharpoons MnO_2 + Mn^{2+} + 4H^+$$

or to corresponding species in alkaline solution.

Considering the instability of the trivalent Mn state, there are two possibilities for interpretation of the decrease of $Mn(OH)_6^{3-}$ concentration in the discharge and recharge process (see Figs 11–13). One is the decomposition of $Mn(OH)_6^{3-}$, another is redeposition of Mn species back to the porous graphite electrode to form $Mn(OH)_2$ (further reduced) in the discharge process and MnO_2 (further reoxidised) in the recharge process. In order to test the stability of dissolved low oxidation-state Mn species in the period of experimental interest, a time-dependence experiment was carried out under the same conditions as those in the electrochemical experiments, the results of which are shown in Fig. 14. The time of observation was up to 5 h, which was the period needed for the single discharge or recharge half-cycles. The absorption is taken at the

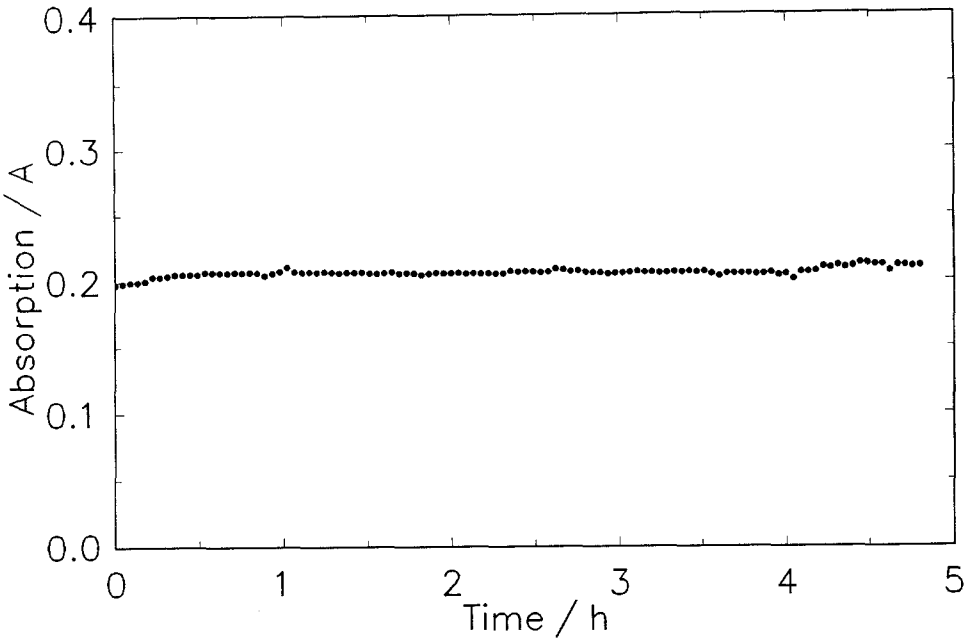

Fig. 14. Lack of change of the absorption of Mn(III) species with time.

maximum absorption wavelength (465 nm). The results show that the low valent Mn species are, in fact, quite stable over the period of time involved in a single discharge/recharge cycle. Hence redeposition with reduction of Mn(III) in cathodic polarization is the main reason for the decrease of the $Mn(OH)_6^{3-}$ concentration. In other words, during the discharge and recharge, the Mn(III) formed in the first electron transfer is soluble under both conditions and further discharge or recharge can drive the soluble species to solid-state $Mn(OH)_2$ or to MnO_2 onto the porous graphite electrode. Since the CM MnO_2 has been proved to be rechargeable, it is logical to expect that the regenerated MnO_2 must be rechargeable, i.e. for CM MnO_2, the soluble Mn(III) species, both in solution or adsorbed on the porous electrode structure, can be reoxidized back to rechargeable MnO_2. The presence of Bi(III) is essential for this behaviour to arise.

It should be emphasised that the $Mn(OH)_6^{3-}$ concentration was stable for 5 h, but this does not necessarily mean that $Mn(OH)_6^{3-}$ is a stable ion over substantially longer periods of time. Actually, in our long-period cycling experiments [35], after two days, solid MnO_2 can be found deposited on the walls of the cell compartment in which the MnO_2 electrode was accommodated, and on the separator. Of course, in a practical cell without 'free electrolyte', such processes are minimized.

There remains another critical question about the soluble species: that is, how much Mn (absolutely) could diffuse into the solution. By means of AAS, the total amount of Mn species which diffused away from the electrode was evaluated quantitatively. Two trials have been done: in the first, all the Mn species including solid MnO_2 on the separator and on the walls of cell, and the $Mn(OH)_6^{3-}$ in the solution were collected. 5% of the total MnO_2 was found diffused into the solution. In the second trial, just $Mn(OH)_6^{3-}$ in the solution was collected. The concentration of Mn(III) was found to be 2.4×10^{-3} M. The saturation concentration was reported as 4.4×10^{-3} M [11]. The amount of the Mn(III) in the solution was equivalent to 2% of total MnO_2. The experiments took approximately 48 h. In the u.v.-visible spectroelectrochemical measurements, the concentration was also found to approach the saturation value.

Based on the *in situ* optical electrochemistry experiments, it is evident that the soluble species are $Mn(OH)_6^{3-}$ and they are formed both in the *cathodic* discharge and in the *anodic* recharge process. The amount of $Mn(OH)_6^{3-}$ in solution increases already quite early in discharge (or recharge) and decreases in further stages of discharge (or recharge). Finally, the quantities of Mn species which diffuse into the solution are determinable quantitatively giving results which show that the solution becomes almost saturated with $Mn(OH)_6^{3-}$ around -0.3 V against HgO/Hg. Considering that the maximum absorption values for both cathodic discharge and anodic recharge processes were almost the same, it can be concluded that in both processes the concentration of $Mn(OH)_6^{3-}$ approaches saturation; this is virtually in agreement with what may be calculated from the extinction coefficient and the known solubility [11, 36]. In long-time cycling experiments, the $Mn(OH)_6^{3-}$ can disproportionate, giving rise to deposits of MnO_2 and $Mn(OH)_2$ on the walls of the cell and separator, or even suspended in the electrolyte.

It appears that most of the 'soluble' species remain adsorbed or absorbed in the porous electrode; the concentration of free $Mn(OH)_6^{3-}$ in the electrolyte can attain the saturation value but, in both the cathodic discharge and the anodic recharge, the soluble $Mn(OH)_6^{3-}$, both in solution and adsorbed on the porous electrode, can become respectively redeposited

as $Mn(OH)_2$ or MnO_2. Obviously, the latter materials can be recharged or redischarged in the CM electrode, so the steps of redeposition could be one of the key processes in the rechargeability. It may be suggested that one of the roles of bismuth is related to the redeposition from the soluble $Mn(OH)_6^{3-}$ (both in solution or adsorbed in the porous electrode), e.g. acting as a nucleation catalyst.

4. Conclusions

(i) From three types of detector experiments, it can be concluded that the soluble Mn(III) species, which were indicated as $Mn(OH)_6^{3-}$, are formed significantly, even at the beginning of a discharge half-cycle in the case of the CM MnO_2, and this behaviour differs from that found with γ-MnO_2.

(ii) The mechanisms of the cathodic and anodic reactions of CM MnO_2 are found to be different from those of γ-MnO_2. The process of 'proton hopping' in the lattice of MnO_2 which is the rate-determining step in the reduction of γ-MnO_2, may be bypassed by the heterogenous mechanism involving production of soluble $Mn(OH)_6^{3-}$ ion. The proposed heterogenous mechanism can provide a reasonable interpretation of the observed phenomena, e.g. the observed relatively flat discharge profile and the much higher current density that can be realized experimentally for CM MnO_2 compared to that for γ-MnO_2 electrodes [35].

(iii) The soluble intermediate, $Mn(OH)_6^{3-}$, plays an important role in the process of discharge/recharge of CM MnO_2. For example, in the RRDE experiments, CM MnO_2 loses its rechargeability if $Mn(OH)_6^{3-}$ is spun away from the disc MnO_2 at high rotation rates.

(iv) The rechargeability of CM MnO_2 relies, in part, on the redeposition of the soluble species. In practical battery embodiments, there would be *no* problems arising from this situation since a restricted electrolyte volume is used and virtually no free liquid electrolyte is present, as it is in the present optical and detector-electrode experiments.

Acknowledgement

Grateful acknowledgement is made to the Natural Sciences and Engineering Research Council of Canada for support of this work on a Strategic Grant. We also thank Dr H. S. Wroblowa for a number of useful discussions on this work.

References

[1] N. C. Cahoon and M. P. Korver, *J. Electrochem. Soc.* **100** (1959) 745.
[2] G. S. Bell and R. Huber, *ibid.* **111** (1964) 1.
[3] A. Kozawa and J. F. Yeager, *J. Electrochem. Soc.* **115** (1968) 1003.
[4] A. Kozawa and R. A. Powers, *ibid.* **113** (1966) 870.
[5] *Idem, Electrochem. Tech.* **5** (1967) 535.
[6] *Idem, J. Electrochem. Soc.* **115** (1968) 122.
[7] A. Kozawa and B. Kagaku, BMRA Symposium, Brussels 38 (1983).
[8] A. Kozawa and J. F. Yeager, *J. Electrochem. Soc.* **112** (1965) 959.
[9] A. Kozawa and R. A. Powers, *J. Chem. Educ.* **49** (1972) 587.
[10] K. J. Vetter, *Z. Elektrochem.* **66** (1962) 577.
[11] A. Kozawa, T. Kalnoki-kis and J. F. Yeager, *J. Electrochem. Soc.* **113** (1966) 405.
[12] K. A. K. Lott and M. C. R. Symons, *ibid.* (1959) 829.
[13] P. Ruetschi, *ibid.* **123** (1976) 495.
[14] J. McBreen, *Power Source* **5** (1975) 525.
[15] P. Ruetschi, *J. Electrochem. Soc.* **135** (1988) 2657.
[16] *Idem, ibid.* **131** (1984) 2737.
[17] P. Ruetschi and R. Govanoli, *ibid.* **135** (1988) 2663.
[18] W. C. Vosburgh and Pao-soong Lou, *ibid.* **108** (1961) 485.
[19] D. Boden, C. J. Venuto, D. Wisler and R. B. Wylie, *ibid.* **114** (1967) 415.
[20] A. Era, Z. Takehara and S. Yoshizawa, *Electrochim Acta* **13** (1968) 207.
[21] J. B. Fernandes, B. D. Desai and V. N. Kamat Dalal, *ibid.* **29** (1984) 181.
[22] H. Y. Kang and C. C. Liang, *ibid.* **115** (1968) 6.
[23] D. Boden, C. J. Venuto, D. Wisler and R. B. Wylie, *ibid.* **115** (1968) 333.
[24] K. Kordesch, J. Gsellmann, M. Peri, K. Tomantschger and R. Chemelli, *ibid.* **26** (1981) 1495.
[25] K. Kordesch, BMRA Symposium, Brussels 81 (1983).
[26] K. Kordesch, J. Daniel-Ivad, E. Kahraman, R. Mussnig and W. Toriser, Paper 910052, 26th International Energy Conversion Engineering Conference. Boston, MA (1991).
[27] S. Fletcher, J. Galea, J. A. Hamilton, T. Tran and R. Woods, *J. Electrochem. Soc.* **133** (1986) 1277.
[28] Xi Xia and Chingwen Li, Extended Abstracts, **1** (91) 28, Electrochemical Society Spring Meeting (1991), Washington, D.C.
[29] Y. F. Yao, N. Gupta and H. S. Wroblowa, *J. Electroanal. Chem.* **223** (1987) 107.
[30] H. S. Wroblowa and N. Gupta, *J. Electroanal. Chem.* **238** (1987) 93.
[31] M. A. Dzieciuch, N. Gupta and H. S. Wroblowa, *J. Electrochem. Soc.* **135** (1988) 2415.
[32] Y. F. Yao, *US Patent 4 520 005* (1985).
[33] M. A. Dzieciuch, H. S. Wroblawa and J. T. Kummer, *US Patent 4 451 543* (1984).
[34] H. S. Wroblawa, N. Gupta and Y. F. Yao, BMSI (1985) 203.
[35] L. Bai, D. Y. Qu, B. E. Conway, Y. H. Zhou and W. A. Adams, *J. Electrochem. Soc.* (1993) in press.
[36] M. Ibers and J. T. Davidson, *J. Amer. Chem. Soc.* **72** (1950) 4744.
[37] R. Drummond and M. Waters, *J. Chem. Soc.* (1953) 435.
[38] J. Fitzpatrick and F. L. Tye, *J. Appl. Electrochem.* **21** (1991) 130.